Solid Freeform Fabrication 2019: Proceedings of the 30th Annual International
Solid Freeform Fabrication Symposium – An Additive Manufacturing Conference
Reviewed Paper

SIMULATION OF HYBRID WAAM AND ROTATION COMPRESSION FORMING PROCESS

Xushan Zhao[1], Yuanxun Wang[1], Guilan Wang[2], Haiou Zhang[3]

[1]School of Cicil Engineering & Mechanics
Huazhong University of Science and Technology, Wuhan 430074, PR China
[2]School of Materials Science and Engineering
Huazhong University of Science and Technology, Wuhan 430074, PR China
[3]School of Mechnical Science & Engineering
Huazhong University of Science and Technology, Wuhan 430074, PR China

Abstract

Wire arc additive manufacturing (WAAM) has been studied and widely applied due to its high forming efficiency and low production cost. In the process of WAAM, there are problems of cracking, deformation, large residual stress, insufficient properties, and instability caused by repeated rapid heating and chilling. Welding with rotation compression can control the performance and shape synchronously in the semi-solidified state of the weld pool. In this study, a new solution of hybrid WAAM and rotation compression is presented using follow-up rotating device to form the weld bead layer by layer. Base on the finite element analysis result of the hybrid process, the force energy curve of the rotation forming metal flowing process is obtained by arranging history monitory points and paths on the bead, and the relationship between the shape and forming load is revealed. The simulation model was verified by forming tests on middle carbon steel.

Keyword： Welding with rotation compression, WAAM, Deformation control, Residual stress

Introduction

Owing to the pattern shift that the process provides over conventional manufacturing，additive manufacturing(AM) has got extensive attention in recent years [1]. AM has the advantages of resource efficiency, environmental friendliness, and the ability to form complex parts against traditional manufacturing. The Wire and Arc Additive Manufacturing (WAAM) is one of AM using electric arc as the heat source and combining wire as raw material. It has been widely studied and applied in the production of large and medium-sized parts over the past few decades due to its high energy efficiency, low cost, and deposition rate comparing with laser or electron beam deposition AM technology [2].

However, there were many adverse effects such as cracking, deformation, large residual stress, insufficient properties and instability caused by the complexity of the WAAM forming process, which may result in the poor quality of the bead.

The freeform deposition conditions, such as manufacturing path, energy power, traverse speed, and cooling methods, have been studied. Many solutions have been proposed to control thermal accumulation and to improve forming semblance of the WAAM such as planning for good fusion paths [3], controlling heat input [4], optimizing forming process [5] and regulating external environmental impact [6], et al. The shaping capability can be improved in certain degree under appropriate deposition conditions [7]. But the problems of deformation and coarse grain are still not well resolved during WAAM process if only relying on a single process.

Hybrid AM Processes are defined as the AM process with compositing more than one manufacturing technology that is fully coupled and synergistically affect part quality, functionality, and process performance. The primary goal for the majority of hybrid-AM processes is improving part quality performance rather than improve processing [8].

As a mature traditional process technology, the milling process has many characteristics such as high flexibility, high precision and easy control. It is the most common composite form with metal additive manufacturing technology, which can effectively improve the surface geometric accuracy of the formed parts. However, the milling process will undoubtedly reduce the utilization rate of the metal material due to removing the material of the formed part again and again, which is not conducive to the advantages of the additive manufacturing technology. It is imperative to find a way to ensure the forming accuracy without spending time milling the molten layer and improving material utilization.

The effect of the pulsed ultrasonic and the continuous ultrasonic on the short-circuiting transfer of GMAW was studied by Chao Chen et al [9-10]. The droplet transfer behavior, the welding electrical signals, and the weld appearance were exploited to characterize the feasibility of the pulsed ultrasonic-assisted GMAW. They fund that hybrid deposition and ultrasonic have a good indicative of decreasing necking and stabling process.

Hybrid welding with trailing hammering (HWTH) was proposed by Fang Hongyuan to improving the stress distribution of welded joints [11-12]. HWTH can control the longitudinal and lateral shrinkage deformation of the welding to a very low level. Besides, it can hammer and strengthen the different parts of the welded joint through improving the stress distribution state of the welded joint to controlling the welding hot crack and the transverse and longitudinal deformation of the weld effectively according to the actual needs.

Hybrid deposition and micro rolling (HDMR) which was applied to improve residual stress and distortion, which can result in the part being out of tolerance and can impede performance [13-14]. Hybrid-AM by rolling solves two key problems in additive manufacturing: alleviate some of these inaccuracies without removing material, undesired residual stress from the building process warps or distorts the final workpiece [8]. But this process is not suitable for parts with complex paths, such as sharp corners.

Hybrid laser-arc welding (HLAW) was used to maintain the high integrity bead and induce gas porosity in the Aluminum alloy manufacture process by Priti Wanjaraa and Xinjin Caob [15], and which has a good promotion in assisting the build process and improving build quality in the welding of high strength steels has been certified by O. Berdnikova, V. Pozniakov and O. Bushma [16]. Unlike the other hybrid processes of additive manufacture, the material deposition and auxiliary lasers are added simultaneously in the same position in hybrid laser-arc welding (HLAW).

Hybrid deposition and laser shock peening (HDLSP) is the combination of arc additive manufacturing process with laser peening. Laser shock peening(LSP) is a surface treatment that dates back to the 1960s where shock waves from rapidly expanding plasma plastically deform a workpiece [8]. The effect of LSP on different materials and confirmed that LSP could induce compressive residual stress and increasing microhardness to improve performance have been investigated [17].

The effect of hybrid welding and impacting rotation(HWIR) on the quality of TC4 thin plate welded joints has been studied by Zhang Y et al [18-19]. The results show that HWIR plays a significant role in improving mechanical properties of welding joint and reducing welding residual stress compared with the conventional welded parts due to the martensite transformation occurs in the weld and the near seam area of the welding and impacting rotator.

Various studies have proved that welding with extruding has a significant improvement in the mechanical properties of the weld bead. Among them, the HWIR process has great advantages: the rotary ram speed and the pressing amount are easy to control, and the rotary ram can flatten the weld bead to improve the precision of the weld bead surface during the pressure welding trajectory when the auxiliary rotating equipment is not affected by the welding trajectory. Taking these advantages into consideration, it will be of significance and great research value to combine the welding rotating process with the metal additive manufacturing process to form a new composite additive manufacturing process.

In this study, a new hybrid metal addictive manufacture process that combines the auxiliary rotation and WAAM was proposed to improving the surface precision of the formed parts, reducing the processing cycle and enhancing the mechanical properties of the formed parts. Hybrid deposition and impacting rotation (HDIR) was modeled in Abaqus to study the effect of impacting rotation on the morphology of welding bead and the changing regularity of temperature field and stress field in the process of hybrid forming.

Model

Heat Source Model Building

In general, the heat source forms used in arc additive manufacturing simulation are mainly divided into three types: a centralized heat source, planar distributed heat source, and volume distributed heat source. The volume heat-source model can reflect the actual arc heat source more than the other two models while the penetration of arc energy over the thickness of the workpiece was considered. During the arc movement in the actual forming, the shape of the instantaneous weld pool is not symmetrical along the Y-axis because the temperature gradient in the first half is steep and the temperature gradient in the second half is slow. The double-ellipsoid-volume heat-source model is used to describe the arc thermal load result from it can accurately describe the heat flow distribution and weld pool shape during actual welding [20].

The double ellipsoid model formula is shown in equation (1), and the double ellipsoid model is shown in Figure 1.

$$\begin{cases} q(\mathrm{x,y,z,t}) = \dfrac{6\sqrt{3} f_f Q}{\pi a_f bc\sqrt{\pi}} \exp\left[\dfrac{-3\xi^2}{a_f^2} + \dfrac{-3y^2}{b^2} + \dfrac{-3z^2}{c^2}\right], & x > 0 \\ q(\mathrm{x,y,z,t}) = \dfrac{6\sqrt{3} f_r Q}{\pi a_r bc\sqrt{\pi}} \exp\left[\dfrac{-3\xi^2}{a_r^2} + \dfrac{-3y^2}{b^2} + \dfrac{-3z^2}{c^2}\right], & x < 0 \end{cases} \tag{1}$$

$$Q=\eta UI\ , \quad \xi = x - vt \tag{2}$$

Where the fractions f_f and f_r of the heat deposited in the front and rear quadrants are needed where $f_f = 0.5, f_r = 1.5$. And the parameters a,b,c can have different values in the front and later quadrants as expressed in [20] since they are independent, and the Q is the thermal energy transferred to the workpiece per unit time, U and I are the arc voltage and welding current, respectively, and η is the arc thermal efficiency. The v is the speed of heat source.

Table 1 Variable of double ellipsoid heat source

Name	a_f	a_r	b	c
Variable(mm)	5	15	5	2.5

The double ellipsoid heat source model used in this paper belongs to the body heat source. Its molten pool is not only distributed in the new layer of weld bead but also remelted in the old layer. The heat source model and the temperature distribution alongthe cross-section of Y-axis of the molten pool position are shown in Figure 1.

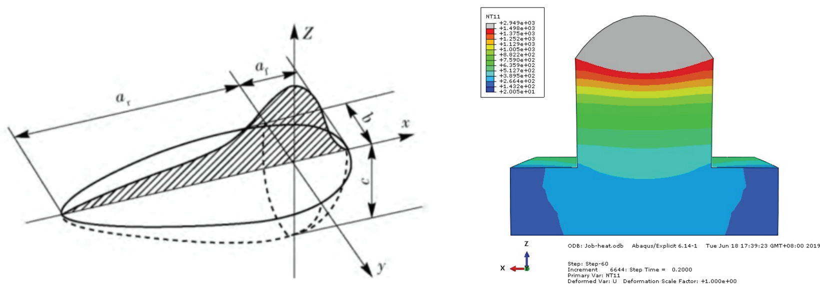

Figure 1 Double ellipsoid heat source model and the Molten pool appearance

Welding Bead Model Building

In this work, several assumptions were made to build the simulation model. The processing material is medium carbon 45# steel. The MIG welding torch is used to conduct additive manufacture in the front, the rotating head is moved in the same direction as the welding torch, and the weld bead is rotated and compressed to control the shape and quality. The schematic view is shown in Figure 2.

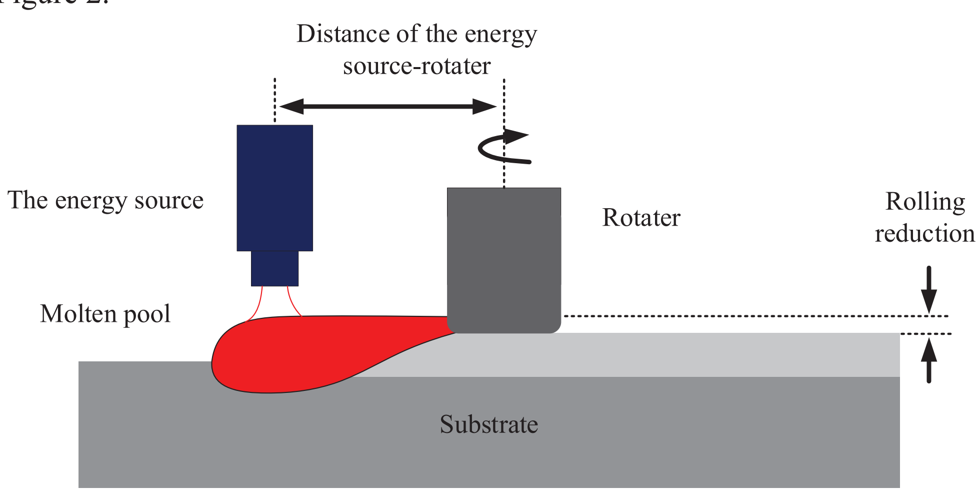

Figure 2 The schematic of WDIR process

Basic assumptions of the model:

(1) The material is isotropic;

(2) The influence of the flow of the molten pool to the temperature field is ignored;

(3) Replace the influence of the substrate fixture on the temperature field of the bead with convection heat;

(4) The latent heat is negligible for the phase change;

(5) The cooling effect of the rotating head is realized by a large heat transfer coefficient that the value is 50.

Parameters of the simulation process

The hybrid arc-rotation additive manufacturing process has multiple influence parameters, including the energy source-rotator distance, rolling reduction, rotational speed, and friction coefficient. In order to explore its influence on the forming quality, the design simulation comparison is shown in the following Table 2. It should be noted that the Job-1 is the free deposited so that its parameters are zero.

Table 2 Simulation list of rotating parameters

Job name	**Job-1**	**Job-2**	**Job-3**	**Job-4**	**Job-5**	**Job-6**	**Job-7**	**Job-8**	**Job-9**	**Job-10**
The energy source-rotator distance (mm)	0	40	35	30	40	40	40	40	40	40
Rotation reduction (mm)	0	0.8	0.8	0.8	0.7	0.6	0.8	0.8	0.8	0.8
Rotating Speed (rad/min)	0	300	300	300	300	300	350	400	300	300
Friction Coefficient	0	0.2	0.2	0.2	0.2	0.2	0.2	0.2	0.15	0.1

For the spinning problem, its convergence is not guaranteed when the mesh is too fine. Therefore, in this study the grid node seed density adjustment is performed to guarantee the efficiency and accuracy of the calculation while considering the convergence. Finally the bead part was composed of 27600 elements, and the rotator includes 8640 elements, as shown in Figure 3. The C3D8R mesh was used to generate the simulation model. With considering the accuracy and calculative efficient of nonlinear large deformation solution, a short model has been used to replace the real manufacture process. The length of the bead is 100mm, and its width is 10mm. This part includes four formed layers that height is 2mm and one new forming layer that height is 2.6mm. The rotator was defined as a rigid part to guarantee the rotating forming simulation, whose maximum radius is 15mm, and the radius of the side of the rotating contact surface is 15mm. Since this paper focuses on the influence of the rotation forming process on the temperature field and the residual stress field, the thickness of the substrate is set to 5mm to avoid excessive influence of the substrate on residual stress.

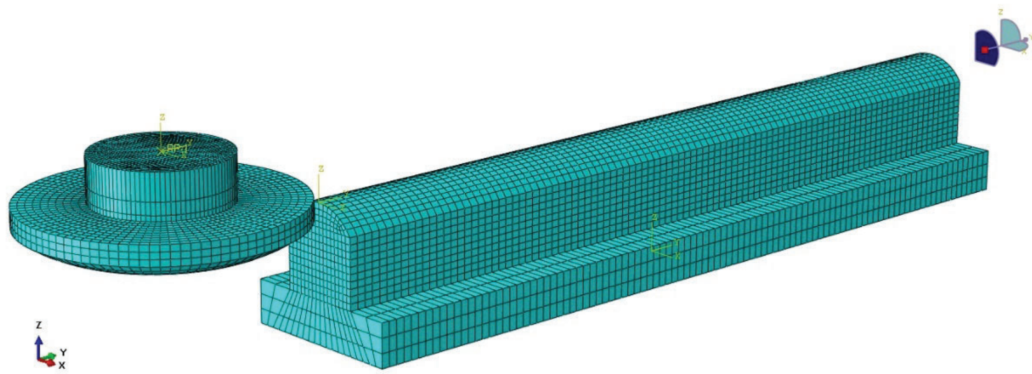

Figure 3 Finite element model of HWID

Initial Condition and Boundary Condition

The initial temperature of the bead and rotator is 20°C. The bottom of the weld bead was fully restrained in the global coordinate system. Except for Y-axis translation and Z-axis rotation, other degrees of freedom of rotator are constrained, and the other parameter was showed in Table 2. The thermal physical parameters are listed in Table 3.

In the HDIR additive manufacturing process, a large portion of the heat loss of the weld bead is caused by contact heat transferred between the weld bead and the rotating head.The expression of contact heat conduction between the weld bead and the rolled piece is:

$$q = \lambda(\partial T / \partial y) = \alpha\left(T - T_g\right) \tag{3}$$

The q is the heat density, and the λ is the thermal convection coefficient. The α is the heat transfer coefficient that the value is 50 W/(m^2·°C), and the T is the temperature of the bead as the T_g is the temperature of the rotator.

During the accumulation and cooling of the HDIR additive manufacturing, the metal material dissipates heat primarily through radiation and convection to the surrounding air. Convection in high temperature areas dominates. Conversely, low temperature areas are dominated by convection. In order to simplify the calculation, a composite heat transfer coefficient was used in the study to comprehensively consider the convection and radiation-induced thermal diffusion.

$$h_c = \frac{\delta\varepsilon\left(T^4 - T_\varepsilon^4\right)}{T - T_\varepsilon} + h_{con} \tag{4}$$

The h_c is the radation heat transfer coefficient and the h_{con} is convective heat transfer coefficient. The δ is the Stefan-Boltzmann constant and the ε is the radation coefficient of the bead material, both values of them are given in Table 3.

Table 3 The list of thermal physical parameters

Parameter	Thermal radiation coefficient	Thermal convection coefficient ($W/(m^2 \cdot °C)$)	Environment temperature (°C)	Stefan-Boltzmann constant (W/m^2K^4)
Value	0.85	0.2	20	5.67×10^{-8}

The fully coupled thermo-mechanical analysis in this paper use uniform, isotropic thermophysical material properties as a function of temperature by [21], The material elastoplastic model uses a follow-up hardening model based on the Mises yield criterion.

For 45# steel, the phase change has a large effect on the material properties. In this study, phase transitions were predicted based on the CCT phase diagram of the material and the estimated cooling rate (t8 / 5: 10 s to 30 s) and the corresponding results were used. Material properties and latent heat of phase change are considered by modifying the specific heat curve[22]. On the other hand, in the region where the temperature is higher than the melting point, the thermal conductivity is artificially increased to 10 times the original value in order to simulate fluid convection heat transfer in the molten pool region [23].

Result

In order to test and verify the simulation of hybrid deposited and impacting rotation (HDIR), the partial basic experiments that include free deposited and HDIR had been done. The melt inert-gas welding(MIG) was applied to the hybrid impacting rotation and WAAM that experimental substrate is made of 20mm thick Q235 plate, and the wire was selected with 1.2 mm middle carbon steel wire of grade er50-6. The composition of substrate and welding wire was list by Table 4, and the process parameters were given by Table 5.

Table 4 Welding wire forming experimental wire and substrate chemical composition table

Material	C	Mn	Si	S	P
45# steel	0.35-0.5	1.40-1.85	0.8-1.15	≤0.035	≤0.025
Q235 steel	≤0.18	0.35-0.80	≤0.30	≤0.04	≤0.040

The welding speed is also the moving speed of rotator, and the gun plate distance that is the space between the welding touch and substrate was fixed in the process of HDIR. Besides, the parameters of Table 5 is remained unchanged to show the contrast of different processes.

Table 5 HDIR Process Parameter Table

Welding speed (mm/min)	**Wire feed speed (m/min)**	**Wire diameter (mm)**	**Voltage (V)**	**Current (A)**	**Gun plate distance (mm)**	**Current mode**
400	7.5	1.2	30.4	195	12	pulse

The basic equipments of this experiment are XKA5040A machine tool, LORCH welding machine, welding torch, mixed protection gas cylinder (10% CO2, 90% Ar), rotating device, etc. The physical diagram of XKA5040A milling machine that was the installation platform of the welding touch and rotator, and LORCH welding machine is shown in Figure 4(b). The rotating device belongs to the equipment independently developed by our team.

(a) (b)

Figure 4 Deflection of welding equipment (a), Deflection of XKA5040A machine tool (b), Deflection of LORCH welding machines

Figure 5 shows that the bead formed by free deposited, and Figure 6 represents that the bead formed by the HDIR process with different reduction. All of them are 100mm in length regardless of the solder tail. Combined with the simulation results, the real bead profile tallies with simulated weld bead results shown in Figure 11(b).

Figure 5 The bead formed by free deposited

(a)

(b)

Figure 6 The bead formed by HDIR process with different reduction(a), R=0.8mm(b), R=0.8mm

The observations were made by cutting the bead along the y-axis, Figure 7 shows that the top of the bead produced by the rotating process is offset to one side compared with the free deposited bead. The rotating forming bead y-axis section is made by cutting the bead of Figure 6(b).

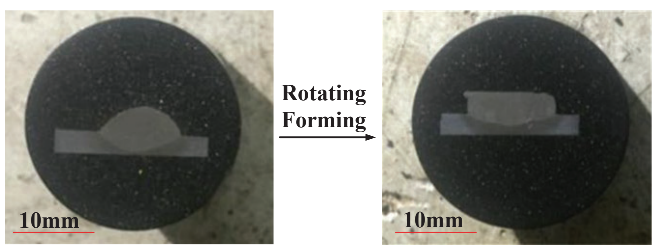

Figure 7 Schematic diagram of the cross-section shape of the experimental forming bead

The rotating head follows the welding torch to rotate the compression bead. Since the temperature near the side of the molten pool is high, the bead profile is directional and biased to one side which is shown in Figure 8.

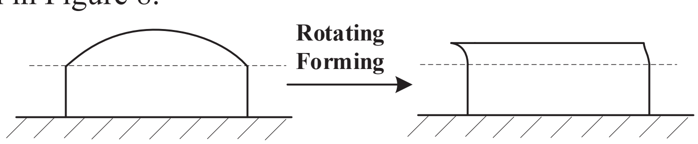

Figure 8 Schematic diagram of the shape change of the bead of rotating forming

In addition to controlling the surface morphology of the weld bead, rotation forming can also change the residual stress distribution, reduce the harmful tensile stress, and enhance the microstructure. As seen in Figure 9, the Mises stress value of the weld bead surface is reduced from 6.5MPa to 5.6MPa.

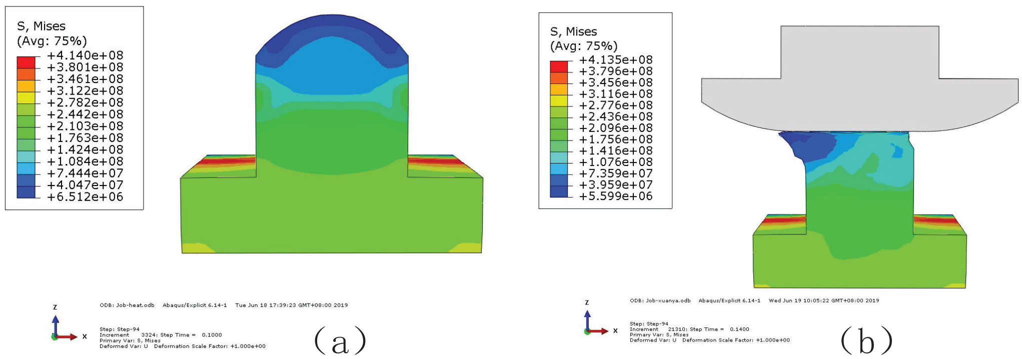

Figure 9 Stress nephogram of y-axis section

(a), Stress nephogram with free deposited (b), Stress nephogram with HDIR

Consider the results of Figure 7 and Figure 8, the accuracy and reliability have been tested and verified by the comparison of the experimental bead cross-section and the simulation y-axis section profile in Figure 9.

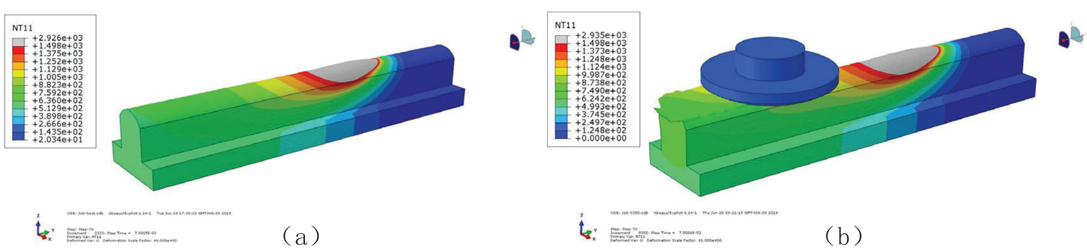

Figure 10 Temperature nephogram of weld bead at step 70

(a), Temperature nephogram with free deposited (b), Temperature nephogram with HDIR

Figure 10 shows the effect of rotator on temperature nephogram of welding bead. The rotator can shape the weld bead shape in the high-temperature zone after the molten pool. At the same time, the temperature in the area after the molten pool is higher than that of free deposition due to frictional heat generation and shaping heat generation.

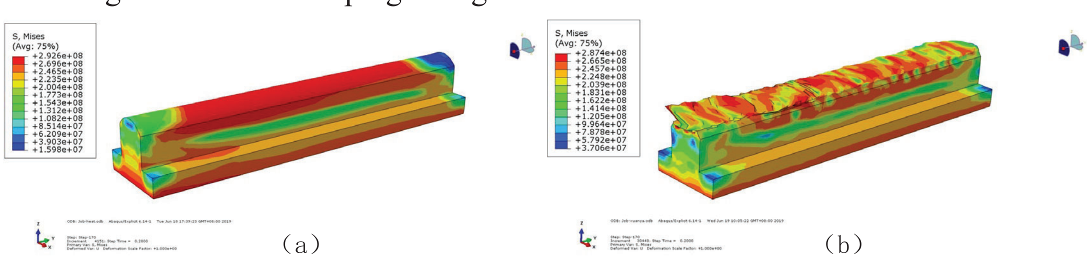

Figure 11 Stress nephogram of weld bead at last step

(a), Stress nephogram with free deposited (b), Stree nephogram with HDIR

One node in the center of the bead upper surface was defined to monitor and analysis the bead temperature, and displacement was shown as Figure 12. Three paths were set up to analysis the stress distribution of the bead. The path x is along the weld bead overlap direction, the path y is along the weld bead fusion direction, and the path z is along the interlaminar depth direction, and their schematic views are as follows:

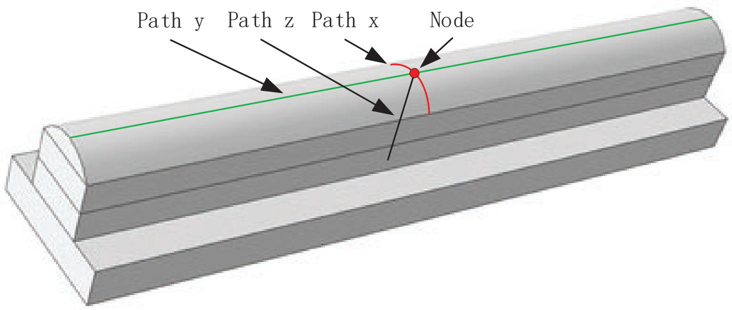

Figure 12 Diagram of three paths and the monitoring node

The path y starts from the beginning to the end of the weld bead in the direction of fusion. The path z starts at the monitoring node of the weld bead and ends at the interface between the weld bead and the substrate.

To analyze the influence of HDIR process on the temperature field, displacement field, and stress field of the weld bead compared with free deposition, the temperature-time curve and displacement-time curve of the monitoring points of free melting and rotation forming are compared and analyzed as shown in Figure 13. Besides, the HDIR in the comparison group is set using the parameters in job-2 which has been shown in Table 2.

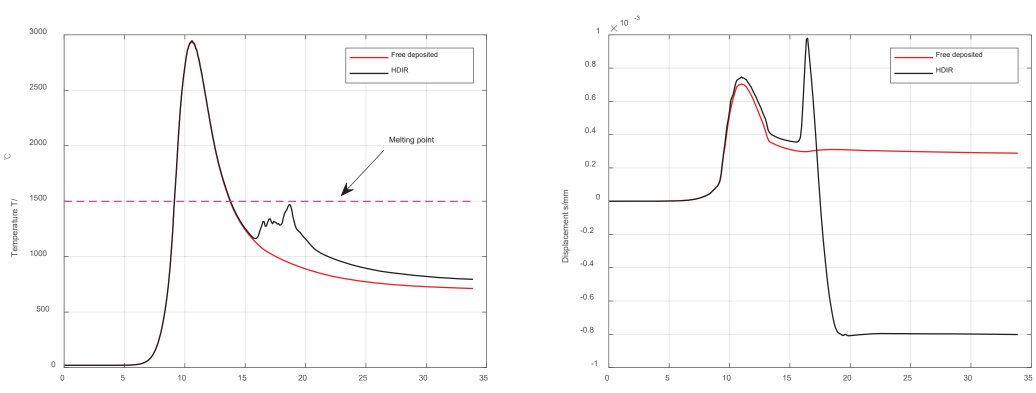

(a) (b)

Figure 13 Effect of HWIR on Temperature; (a), Temperature curves of free deposited and HDIR (b), Displacement curves of free deposited and HDIR

As can be seen from Figure 13, the rotator head has an obvious effect on the weld bead temperature due to frictional heat generation and deformation, but it does not exceed the melting point. Similarly, the HDIR forming will produce a curve peak of U3 displacement due to the pressing of the rotator in the direction of the weld, and then rapidly decrease to the amount of reduction.

The purple boundary line is set to indicate a weld bead having a basic width of 10 mm and a basic length of 100mm so that the influence of the stress of the rotation forming in the effective forming region can be more clearly expressed. Figure 14 depicts the effect of HDIR forming process on principal stress. Three principal stress all be cut down evidently, and the average value of s33 stress even reduced from tensile stress to compressive stress.

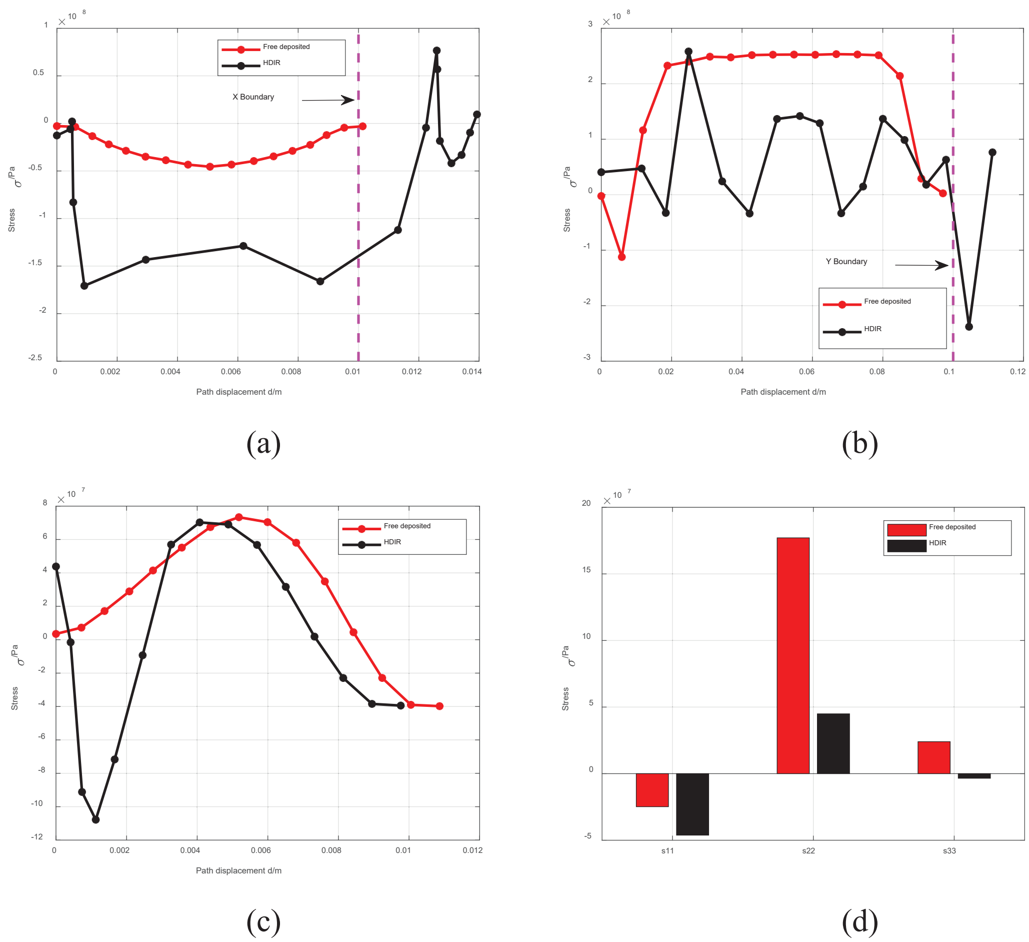

Figure 14 Comparison of stress between free deposited with HDIR (a), the stress s11 in path x (b), the stress s22 in path y (c), the stress s33 in path z (d), the comparison of the average value of stress.

The effect of energy source-rotator distance

The temperature of the rotating forming region is a significant factor for forming accuracy and quality. Moreover, the important variable that controls the temperature of the rotating zone is the energy source-rotator distance. Three level values of energy source-rotator distance were fitted to explore the effect of energy source-rotator distance on manufacture shape and quality.

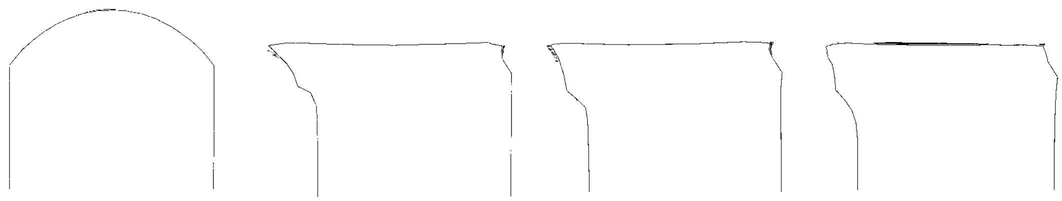

(a) (b) (c) (d)

Figure 15 Comparison of cross-section contours of weld bead after rotating under simulation results with different energy source-rotator distance. (a),free deposited (b),d=40mm (c),d=35mm (d),d=30mm

In this paper, the outline of the Y-axis cross-section of the weld bead after energy source-rotator distance forming is extracted by Matlab as shown in Figure 15 to compare the effect of the energy source-rotator distance in HDIR forming process on the control of the weld bead. Figure 15 shows that the higher the temperature of the forming area, the better the shaping effect, and the less the deviation of the bead to one side. The fundamental reason is that the deformation ability of metals increases with temperature.

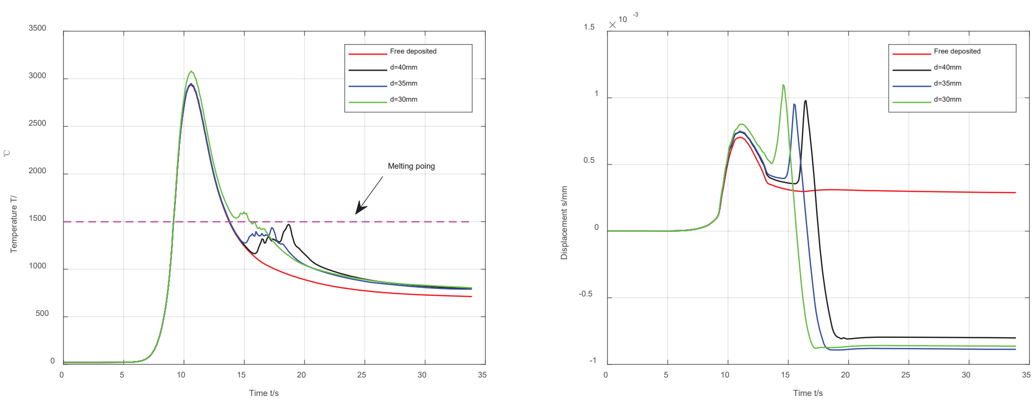

(a) (b)

Figure 16 Effect of the energy source-distance (a), Temperature curves of different energy source-rotator distance (b), Displacement curves of different energy source-rotator distance.

Figure 16(a) shows that the closer the forward roll distance is before the rotating head contacts the molten pool, the more obvious the increase of the temperature field after welding. However, when the rotating head touches the molten pool, the closer the energy source-distance is, the smaller the increase of the temperature field after welding. Furthermore, the peak temperature of the molten pool increases obviously. Figure 16(b) shows that the peak value of U3 curve of job-4 displacement is obviously larger than that of job-2 and job-3, because of its rotating area contacts the molten pool, which makes it easy to deform, while the post-weld displacement has no obvious difference because of its elastic rebound.

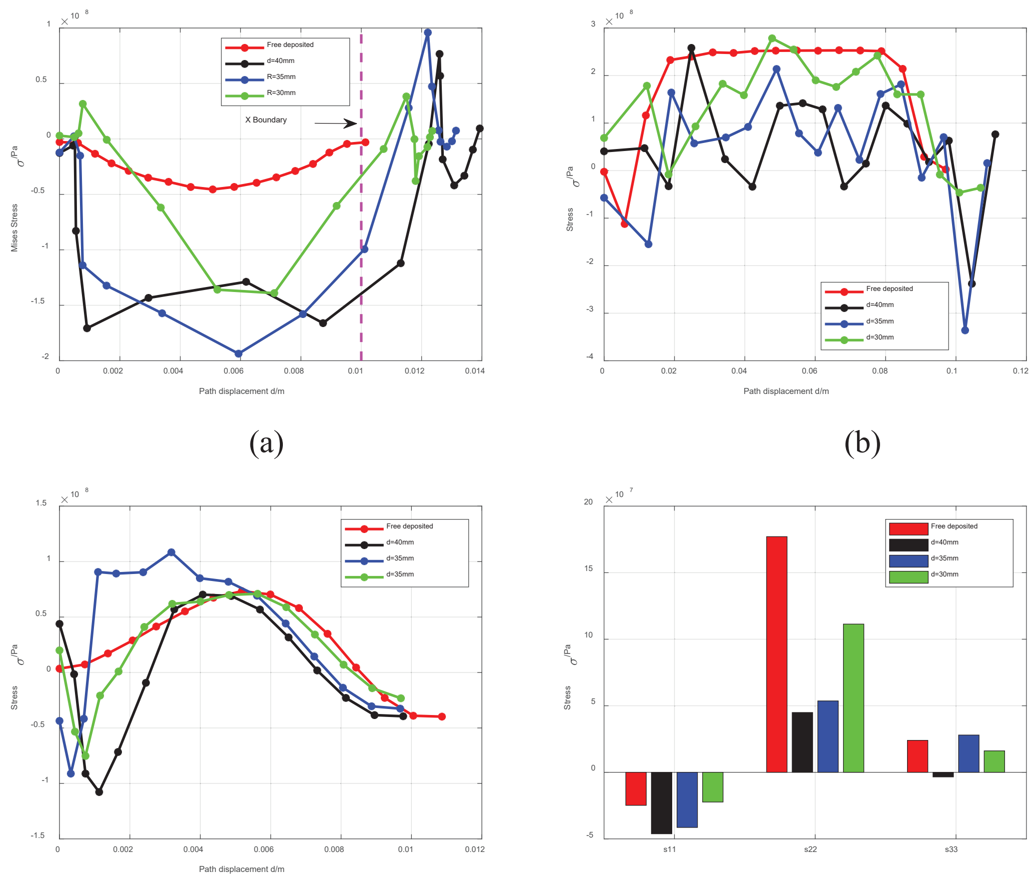

(a) (b)

(c) (d)

Figure 17 The effect of energy source-rotator distance on stress. (a), the stress s11 in path x (b), the stress s22 in path y (c), the stress s33 in path z (d), the comparison of the average value of stress

The results can be summed from Figure 17 that the front roll pitch that is too close in terms of improving the residual stress is less than ideal instead. It is because the yield strength is different due to the difference in temperature. In the case where the amount of reduction is the same, the lower the compression force required for the temperature of the forming region, the more the stress reduction effect is.

The effect of reduction

The reduction refers to the z-axis displacement of the compression bead of the rotating head as shown in Figure 2, which has a direct impact on weld bead deformation. Figure 18 and Figure 19(b) shows the effect of reduction that the amount of deformation is positively related to the amount of reduction. The deformation of the weld bead is prominently displayed on one side due to the different temperature of the front and rear contact areas of the rotating head.

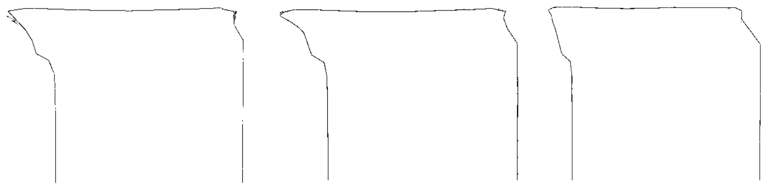

(a) (b) (c)

Figure 18 Comparison of cross-section contours of weld bead after rotating under simulation results with different reduction;(a), R=0.8mm (b), R=0.7mm (c), R=0.6mm.

Figure 19 shows that the greater the amount of reduction, the greater the heat of shaping deformation; the resulting higher temperature peaks. However, compared with the arc heat input, the influence of the deformation heat caused by the reduction amount is small, so the temperature amplitude of the cooling stage tends to be uniform. Both the peak value of the deformation field and the final Z-direction displacement increase with the increase of the reduction amount.

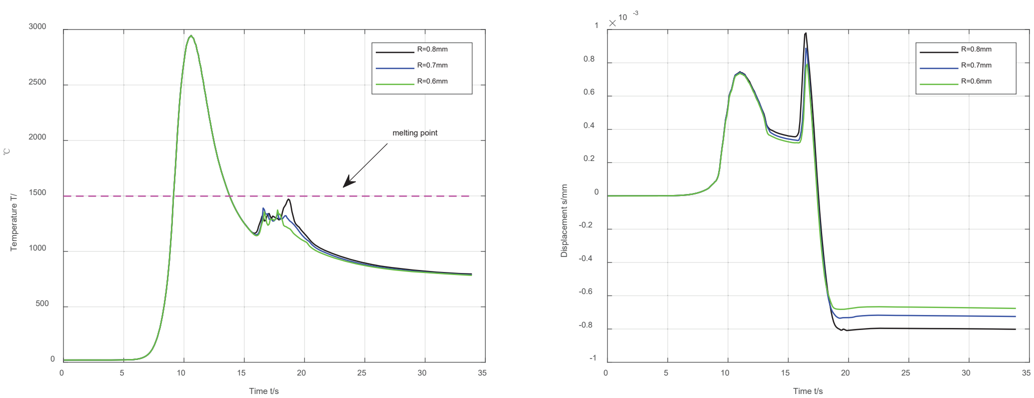

(a) (b)

Figure 19 Effect of Rotation Reduction(a), Temperature curves of different reduction(b), Displacement curves of different reduction.

Figure 20 shows that the reduction has an obvious role in the improvement of the residual stress field. The three principal stresses are all significantly reduced, and the magnitude of the decrease is positively correlated with the amount of reduction which was shown clearly in Figure 20 (d). Furthermore, the z-axis principal stress is even transformed from harmful tensile stress into beneficial compressive stress when the amount of reduction increases to R = 0.8 mm.

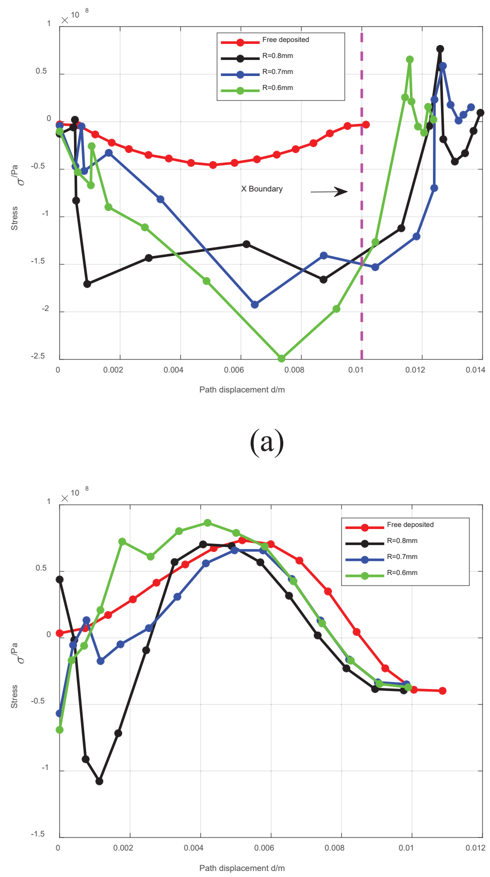

(c) (d)

Figure 20 The effect of reduction on stress (a), the stress s11 in path x (b), the stress s22 in path y (c), the stress s33 in path z (d), the comparison of the average value of stress.

The effect of rotational speed

The rotational speed has a great influence on the shape of the weld bead. The increase of the rotational speed will lead to an increase of the weld bead offset. The embodiment in the outline is shown in Figure 21.

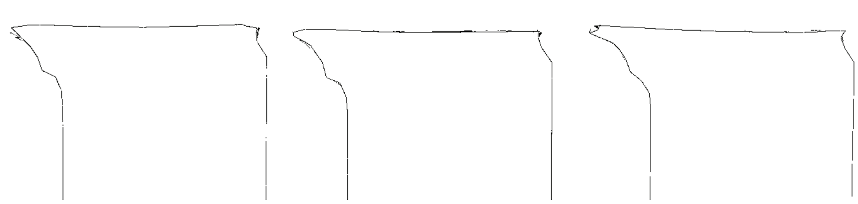

(a) (b) (c)

Figure 21 Comparison of cross-section contours of weld bead after rotating under simulation results with different rotational speed(a),ω=300r/min (b), ω=350r/min (c), ω=400r/min

The rotation speed has little effect on the peak value of the monitoring point temperature curve, but the overall amplitude is positively correlated with the rotating speed. Moreover, the increase in rotating speed promotes the deformation of the weld bead and leads to a larger final displacement of the z-direction.

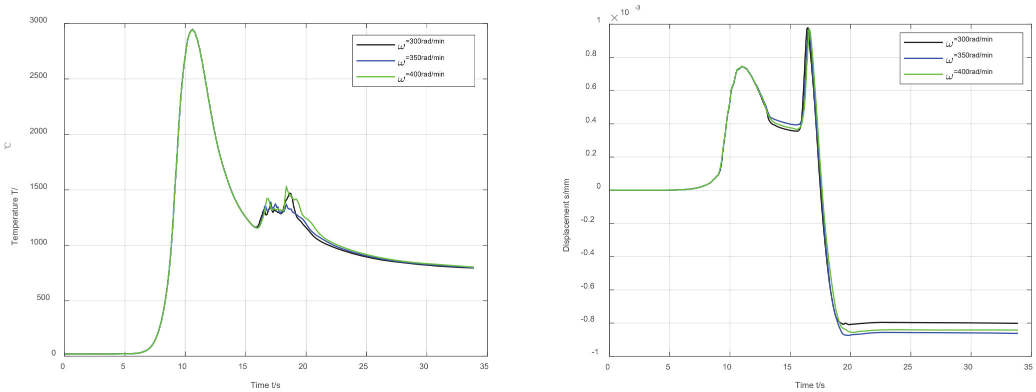

(a) (b)

Figure 22 Effect of Rotating Speed(a), Temperature curves of different rotational speed(b), Displacement U3 curves of rotational speed.

The effect of the rotational speed on the residual stress is mainly reflected in the improvement of the x-axis residual stress of the weld bead. And the increase of the rotating speed will make the x-direction principal stress larger that is compressive stress under the rotating process but has less influence on the z-axis principal stress of the y-axis principal stress.

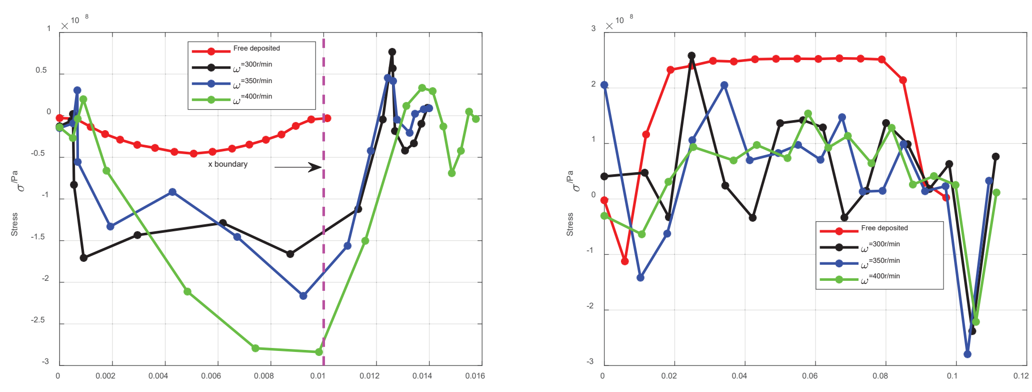

(a) (b)

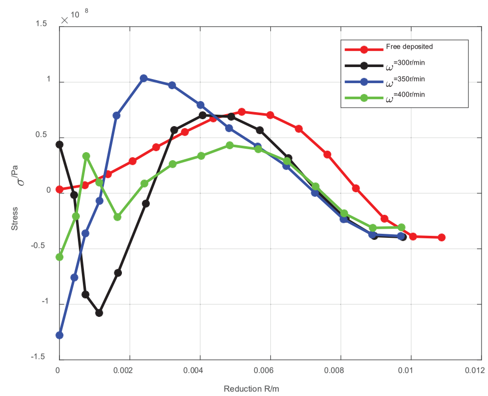

(c)

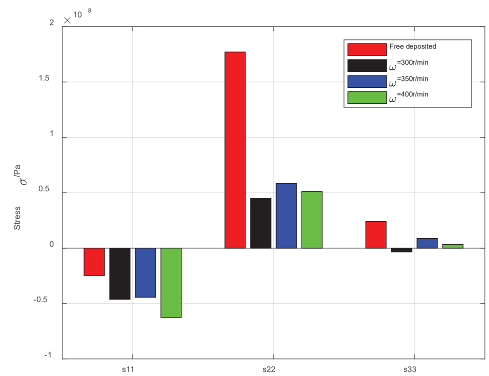

(d)

Figure 23 The effect of the rotational speed on stress (a), the stress s11 in path x (b), the stress s22 in path y (c), the stress s33 in path z (d), the comparison of the average value of stress

The effect of friction coefficient

The coefficient of friction of the rotatning contact surface has an essential influence on the deformation of the weld bead. The lateral deformation of the weld bead is positively correlated with the increase in friction because of the frictional action.

The shape of the weld bead is better as the friction becomes smaller as Figure 24 shows. Because the frictional force in the opposite direction before and after the rotator can bring more uniform weld bead deformation when the other parameters such as the temperature and the reduction of the rotating zone are fixed.

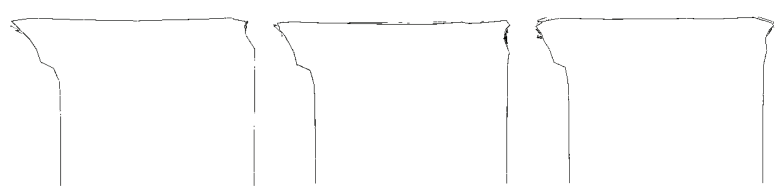

(a) (b) (c)

Figure 24 Comparison of cross-section contours of weld bead after rotating under simulation results with different friction coefficients. (a),f=0.2 (b), f=0.15 (c), f=0.1

It can be seen from Figure 25 that an increase in the friction coefficient leads to an increase in the peak value of the monitoring point temperature curve and a decrease in the z-axis deformation of the final bead due to an increase in frictional heat generation.

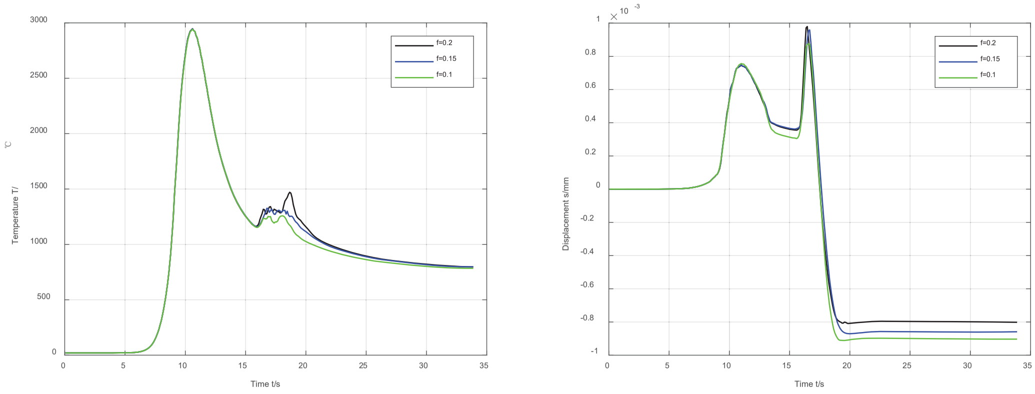

(a) (b)

Figure 25 Effect of Friction Coefficient(a), Temperature curves of different reduction(b), Displacement curves of different reduction.

In terms of the effect of the friction coefficient on the residual stress of the rotating forming, it can be seen from Figure 26 that a high level of friction coefficient has a good influence on the principal stress of x-axis and z-axis. However, a lower friction coefficient can result in a better residual stress improvement for the y-axis principal stress.

The rotating process can greatly improve the residual stress field of the weld bead, which can change the principal stress in three directions from the harmful tensile stress to the compressive stress, or reduce the large tensile residual stress, or make the compressive stress larger. Considering the four factors of the energy source-rotator distance, reduction, rotational speed, and friction coefficient, the influence of the energy source-rotator distance and reduction on the residual stress of the weld bead is quite obvious.

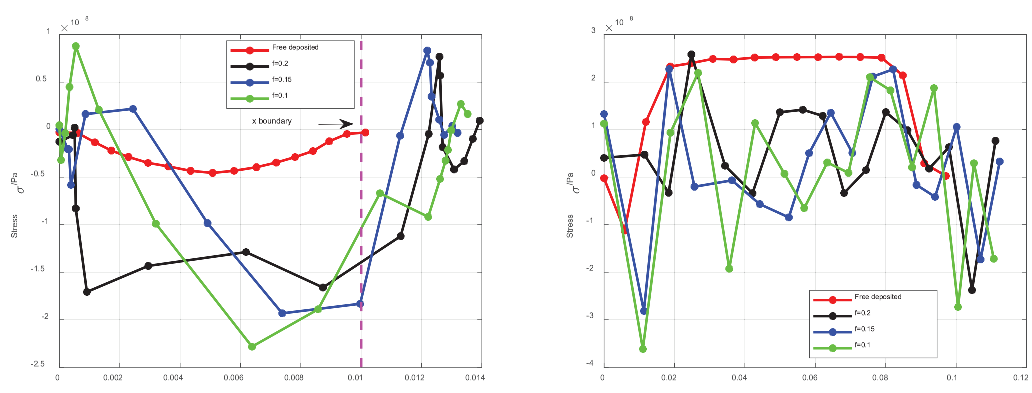

(a) (b)

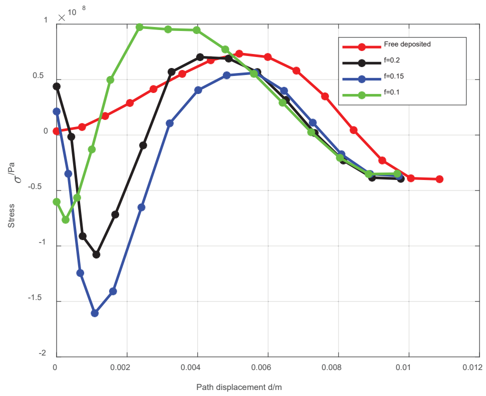

(c)

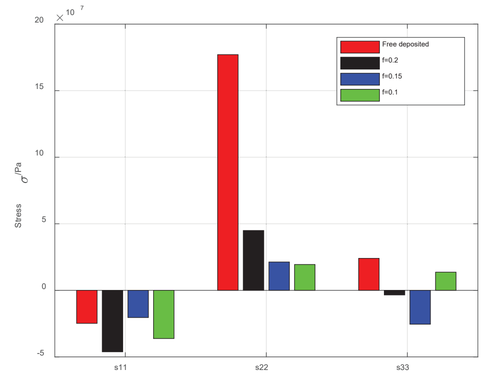

(d)

Figure 26 The effect of the friction coefficient on stress s11 in Path x. (a), the stress s11 in path x (b), the stress s22 in path y (c), the stress s33 in path z (d), the comparison of the average value of stress

In summary, it is summarized from the simulation results that the rotating process can smooth the bead surface and improve the residual stress field by rotating and compression the new layer of the weld bead.

Conclusion

With combining the rotating process of welding with the WAAM process，this paper proposes a new composite metal additive manufacturing technology based on the technical concept of welding and arc welding additive manufacturing. A finite element model was built to investigate the effects of HDIR process parameters, including the energy source-rotator distance, rotating reduction, rotating speed, and coefficient of friction by using Abaqus and Matlab. Combined with the experiment, the simulation results were investigated, and the effect of HDIR principle parameters on temperature and residual stress were discussed in the simulation. The main conclusion was shown as follows:

(1) A new type of hybrid metal additive manufacturing technology was proposed, which can eliminate residual stress in the weld bead and improve weld bead profile. And the feasibility of the technology was verified by basic experiments and finite element simulation.
(2) The simulation results show that the HDIR process can improve bead profile and reduce harmful residual stress. Moreover, the reduction and the distance of source-rotator play a significant part in optimizing residual stress field. The rotating speed has an important effect on perfecting x-axis residual stress s11 and the friction coefficient has a positive correlation effect on reducing residual stress s22 and s33.

(3) The basic experiment of HDIR process was done to investigate the feasibility of this new HDIR process technology. Besides, the actual bead profile can certificate the correctness of the finite element model.

The model is relatively simple and contains certain limiting assumptions. Furthermore, the experiment is extraordinary basic and scattered; however, the model is very simple and crude when combined with experiments which can be further studied to analyze the microstructure to verify whether the rotating process can refine the grains. In the further, the related work, including further systematic experiments and simulations, can be further studied to develop this new hybrid metal additive manufacturing technology.

Reference

[1] Hofmann D C , Roberts S , Otis R , et al. Developing Gradient Metal Alloys through Radial Deposition Additive Manufacturing[J]. Scientific Reports, 2014, 4.

[2] Karunakaran K P , Suryakumar S , Pushpa V , et al. Low cost integration of additive and subtractive processes for hybrid layered manufacturing[J]. Robotics and Computer-Integrated Manufacturing, 2010, 26(5):490-499.

[3] Ding D , Pan Z , Cuiuri D , et al. A practical path planning methodology for wire and arc additive manufacturing of thin-walled structures[J]. Robotics and Computer-Integrated Manufacturing, 2015, 34:8-19.

[4] Long R . Effects of Substrate Preheating on Thermal Stress during Laser Metal Deposition Shaping[J]. Journal of Mechanical Engineering, 2009, 45(10):241.

[5] Fu Y, Wang G, Zhang H, et al. Optimization of surface appearance for wire and arc additive manufacturing of Bainite steel[J]. International Journal of Advanced Manufacturing Technology, 2016:1-13.

[6] Xiaoyu C , Sanbao L , Murphy A B , et al. Influence of helium content on a ternary-gas-shielded GMAW process[J]. Welding in the World, 2018.

[7] Zhang H , Wang X , Wang G , et al. Hybrid direct manufacturing method of metallic parts using deposition and micro continuous rolling[J]. Rapid Prototyping Journal, 2013, 19(6):387-394.

[8] Sealy MP, Madireddy G, Williams RE, Rao P, Toursangsaraki M. Hybrid Processes in Additive Manufacturing. ASME. J. Manuf. Sci. Eng. 2018;

[9] Chao C , Sanbao L , Chenglei F , et al. Feasibility analysis of pulsed ultrasonic for controlling the GMAW process and weld appearance[J]. The International Journal of Advanced Manufacturing Technology, 2018.

[10] Chen, C., Fan, C., Lin, S., Cai, X., Zhou, L., Ye, S., & Yang, C.. Effect of ultrasonic pattern on weld appearance and droplet transfer in ultrasonic assisted MIG welding process. Journal of Manufacturing Processes, (2018) 35, 368–372.

[11] Fang Hongyuan, Dong Zhibo, Xu Wenli. Process of avoiding welding hot cracking of thin plate with trolling peening. Welding & Joining, 2002 (3): 17-20

[12] Xu Wenli, Dawn, Liu Xuesong, et al. Dynamic low stress-little distortion-hot crack free welding technology by trailing peening, [J]. Journal of Materials Science and Technology, 2001, 9(1).

[13] Colegrove P A , Donoghue J , Martina F , et al. Application of bulk deformation methods for microstructural and material property improvement and residual stress and distortion control in additively manufactured components[J]. Scripta Materialia, 2016:S1359646216305267.

[14] Fu Y., Zhang H., Wang G, Wang H. Investigation of mechanical properties for hybrid deposition and micro-rolling of bainite steel[J]. Journal of Materials Processing Technology, 2017, 250, 220–227.

[15] Wanjara P , Cao X J . Hybrid Laser-Arc Welding of AA6061-T6 Butt Joints[J]. Materials Science Forum, 2014, 783-786:6.

[16] Berdnikova O , Pozniakov V , Bushma O . Laser and Hybrid Laser-Arc Welding of High Strength Steel N-A-XTRA-70[C]// Materials Science Forum. Trans Tech Publications, 2016.

[17] Sealy, M. P., Madireddy, G., Li, C., and Guo, Y. B., 2016, “Finite Element Modeling of Hybrid Additive Manufacturing by Laser Shock Peening,” Solid Freeform Fabrication Symposium (SFF), Austin, TX, Aug. 8–10, pp. 306–316.

[18] Zhang Y , Yang J G , Liu X S , et al. Finite Element Analysis of Transient Welding Stress and Strain during Ti-6Al-4V Thin Plate Welding with Impact Rotation[C]// Materials Science Forum. 2012.

[19] Zhang Y , Yang J G , Liu X S , et al. Finite element analysis of controlling the TC4 thin plate weldment wave-like deformation by welding with impacting rotation[J]. China welding,2010,19(4)：74-78.

[20] Goldak J , Chakravarti A , Bibby M . A new finite element model for welding heat sources[J]. Metallurgical and Materials Transactions B, 1984, 15(2):299-305.

[21] Xingwang Bai. Numerical study on arc melting deposition with external electromagnetic field [D]. Huazhong University of Science and Technology, 2014.

[22] Ferro P, Porzner H, Tiziani A, et al. The influence of phase transformations on residual stresses induced by the welding process - 3D and 2D numerical models[J]. Modelling And Simulation In Materials Science And Engineering, 2006, 14(2): 117-136.

[23] Heinze C, Schwenk C, Rethmeier M. Effect of heat source configuration on the result quality of numerical calculation of welding-induced distortion[J]. Simulation Modelling Practice and Theory, 2012, 20(1): 112-123.